# Myeloid/Microglial Driven Autologous Hematopoietic Stem Cell Gene Therapy Corrects a Neuronopathic Lysosomal Disease

Ana Sergijenko[1], Alexander Langford-Smith[1], Ai Y Liao[1], Claire E Pickford[2], John McDermott[1], Gabriel Nowinski[1], Kia J Langford-Smith[1], Catherine LR Merry[2], Simon A Jones[3], J Edmond Wraith[3], Robert F Wynn[4], Fiona L Wilkinson[1] and Brian W Bigger[1]

[1]*Stem Cell & Neurotherapies, Institute of Human Development, Faculty of Medical and Human Sciences, University of Manchester, Manchester, UK;* [2]*Stem Cell Glycobiology, School of Materials, University of Manchester, Manchester, UK;* [3]*Genetic Medicine, St Mary's Hospital, Manchester, UK;* [4]*Blood and Marrow Transplant Unit, Royal Manchester Children's Hospital, Manchester, UK*

Mucopolysaccharidosis type IIIA (MPSIIIA) is a lysosomal storage disorder caused by mutations in N-sulfoglucosamine sulfohydrolase (SGSH), resulting in heparan sulfate (HS) accumulation and progressive neurodegeneration. There are no treatments. We previously demonstrated improved neuropathology in MPSIIIA mice using lentiviral vectors (LVs) overexpressing SGSH in wild-type (WT) hematopoietic stem cell (HSC) transplants (HSCTs), achieved *via* donor monocyte/microglial engraftment in the brain. However, neurological disease was not corrected using LVs in autologous MPSIIIA HSCTs. To improve brain expression *via* monocyte/microglial specificity, LVs expressing enhanced green fluorescent protein (eGFP) under ubiquitous phosphoglycerate kinase (PGK) or myeloid-specific promoters were compared in transplanted HSCs. LV-CD11b-GFP gave significantly higher monocyte/B-cell eGFP expression than LV-PGK-GFP or LV-CD18-GFP after 6 months. Subsequently, autologous MPSIIIA HSCs were transduced with either LV-PGK-coSGSH or LV-CD11b-coSGSH vectors expressing codon-optimized SGSH and transplanted into MPSIIIA mice. Eight months after HSCT, LV-PGK-coSGSH vectors produced bone marrow SGSH (576% normal activity) similar to LV-CD11b-coSGSH (473%), but LV-CD11b-coSGSH had significantly higher brain expression (11 versus 7%), demonstrating improved brain specificity. LV-CD11b-coSGSH normalized MPSIIIA behavior, brain HS, GM2 ganglioside, and neuroinflammation to WT levels, whereas LV-PGK-coSGSH partly corrected neuropathology but not behavior. We demonstrate compelling evidence of neurological disease correction using autologous myeloid driven lentiviral-HSC gene therapy in MPSIIIA mice.

*Received 24 January 2013; accepted 30 May 2013; advance online publication 16 July 2013. doi:10.1038/mt.2013.141*

## INTRODUCTION

Mucopolysaccharidosis type IIIA (MPSIIIA) is a neurodegenerative lysosomal storage disease caused by mutations in the N-sulfoglucosamine sulfohydrolase (SGSH) gene, resulting in a deficiency in the enzyme SGSH (EC 3.10.1.1).[1] SGSH deficiency leads to accumulation of highly sulfated heparan sulfate (HS), resulting in cellular and organ dysfunction, particularly in the brain.[1–4] Patients present in the first decade of life, with progressive failure to achieve developmental milestones, severe behavioral changes, including hyperactivity and sleep disturbances, and cognitive and later motor function decline with death in the second decade of life, although disease severity varies significantly.[1,5,6] Disease neuropathology involves multiple factors including HS storage and sulfation,[2–4] secondary storage substrates,[4,7,8] neuroinflammation,[4,9–12] synaptic changes,[4] and possibly others.

There is no treatment for MPSIII, however, patients with MPSI Hurler, a similar lysosomal storage disorder, often receive hematopoietic stem cell (HSC) transplant (HSCT).[13–16] Donor HSCs repopulate the recipient and secrete enzyme which cross-corrects cells in the periphery. Enzyme cannot cross the blood–brain barrier; however, monocytes traffic from the blood into the brain where they differentiate into microglial cells and mediate cross-correction in the central nervous system.[17] If treated early in life, HSCT mediates significant improvements in cognitive function, life expectancy, and peripheral joint and bone disease in MPSI patients.[13,14,16] HSCT in MPSIIIA patients results in increased lifespan but no significant neurological correction,[18–20] and HSCT produces similar results in MPSIIIA mice.[3]

Several lines of evidence suggest that HSCT treatment failure in MPSIIIA is due to insufficient enzyme produced by donor-derived microglia in the brain. Studies in other neurological metabolic diseases have shown that *ex vivo* lentiviral transduction of autologous HSCs with a missing transgene can correct most of the pathological features of the mouse model of MPSI,[21] where HSCT was less effective, and also metachromatic leukodystrophy, where 10% of normal brain enzyme and neuronal correction was achieved.[22] These preclinical studies in neurological diseases have

*The first two authors contributed equally to this work.*

***Correspondence:*** *Brian W Bigger, Stem Cell & Neurotherapies, School of Biomedicine, Faculty of Medical and Human Sciences, University of Manchester, 3.721 Stopford Building, Manchester, M13 9PT, UK. E-mail: brian.bigger@manchester.ac.uk*

resulted in ongoing clinical trials in metachromatic leukodystrophy and X-linked adrenoleukodystrophy[23] among others soon to commence.

In a previous work, we demonstrated partial neurological correction of MPSIIIA mice using lentiviral-transduced wild-type (WT) cells; but lentiviral-transduced autologous MPSIIIA cells (autologous lentiviral (LV)-HSC gene therapy) were unable to mediate neurological correction, and this appears to be due to insufficient enzyme production in the brain.[3] Complete normalization of neuronal pathology coupled with behavioral normalization has never been achieved in this mouse model to our knowledge. We hypothesized that improving monocyte/microglial enzyme expression could make autologous HSC gene therapy more brain specific and efficient, thus correcting neurological disease in MPSIIIA mice.

Here, we report that the myeloid-specific CD11b promoter, in the clinically relevant pCCL LV,[24] mediates increased monocyte-specific enhanced green fluorescent protein (eGFP) expression over ubiquitous phosphoglycerate kinase (PGK) or myeloid CD18 promoters in HSCT. Furthermore, transduction of autologous MPSIIIA HSCs with a LV expressing codon-optimized SGSH under CD11b, mediated normalization of abnormal open-field behavior, brain HS, secondary storage, lysosomal compartment size, and neuroinflammation in MPSIIIA mice, whereas a PGK driven vector could only mediate partial correction in many of these parameters. Increased monocyte expression resulted in improved brain enzyme without changing peripheral enzyme overexpression, making the CD11b vector potentially safer and more target specific for the brain. We report neurological correction of the MPSIIIA mouse model that is achieved with a clinically relevant protocol and vector copy numbers (VCNs) of 1.2 per cell *via* autologous LV-HSC gene therapy.

## RESULTS

### The CD11b promoter increases lentiviral eGFP expression in CD11b$^+$ and CD19$^+$ peripheral blood leukocytes 6 months after transplantation of gene-modified HSCs

In order to improve brain-targeted gene expression for the primarily neurological presentation of MPSIIIA, we constructed LVs containing eGFP under the myeloid-specific human CD18 (LV-CD18) or CD11b (LV-CD11b) promoters, or the ubiquitous human PGK-1 promoter (LV-PGK) (**Figure 1a**),[25,26] using the pCCL backbone.[24] Monocyte/macrophage lineages express high levels of CD11b and CD18 peripherally and also within the brain where they engraft as microglial cells. Lineage-depleted WT murine bone marrow was transduced *ex vivo* with these vectors and transplanted into WT mice (**Figure 1b**). Colony-forming unit (CFU) potential and % transduction of cells were also assessed (**Supplementary Figure S1a–d**). Donor peripheral blood chimerism, between 94 and 100%, was achieved 6 months post-transplantation (**Figure 1c**). On average, 79–87% donor cells were eGFP$^+$ with no significant differences between promoters (**Figure 1c**). The VCN was significantly higher with LV-CD18 than either LV-CD11b ($P = 0.01$) or LV-PGK ($P = 0.0001$) with no significant difference in copy number between the latter two promoters (**Figure 1c**). The eGFP expression in leukocytes, 24 weeks post-transplant, was significantly higher in LV-CD11b–transduced peripheral blood leukocytes than LV-CD18 ($P = 0.0004$) or LV-PGK ($P = 0.03$) (**Figure 1d**) with significantly higher expression by LV-CD11b in CD11b$^+$ cells compared with LV-CD18 ($P = 0.000077$) or LV-PGK ($P = 0.003$) and in CD19$^+$ cells compared with LV-CD18 ($P = 0.000017$) and LV-PGK ($P = 0.0014$) (**Figure 1e**). The CD11b promoter yielded the highest mean fluorescent intensity:VCN ratio in CD11b$^+$ cells, while the CD18 promoter had the lowest (**Supplementary Figure S1e–g**). Comparison of LV-CD11b– and LV-PGK–transduced mice with similar copy numbers revealed equivalent levels of eGFP expression, except in CD11b$^+$ cells where CD11b promoter expression was significantly (67%) higher than PGK (**Figure 1f–h**). LV-eGFP–transduced donor cells with microglial morphology were readily detected in the brain (**Supplementary Figure S1h**).

### Codon optimization enhances human SGSH activity in a human microglial cell line

Human SGSH cDNA and codon-optimized human SGSH (coSGSH) cDNA were cloned into pCCL LV under either the human CD11b or PGK promoter (**Figure 2a**). Relative SGSH activity was assessed *in vitro* by transiently transfecting the human CHME3 microglial cell line with plasmids containing human SGSH or coSGSH under the ubiquitous PGK promoter (**Figure 2b** and **Supplementary Figure S2a,b**). Codon optimization significantly ($P = 0.0001$) increased SGSH activity by 50% in microglial cells.

### *Ex vivo* autologous LV-HSC gene therapy in MPSIIIA mice is safe and efficient

In order to determine if *ex vivo* transduction of MPSIIIA HSCs can effectively treat the mouse model of MPSIIIA, MPSIIIA HSCs were transduced with the myeloid-enhanced LV-CD11b-coSGSH vector (LV-CD11b) or ubiquitous LV-PGK-coSGSH (LV-PGK) vector and transplanted into busulfan myeloablated 6- to 8-week-old female MPSIIIA mice ($n = 15$) (**Figure 2c**). WT and MPSIIIA littermate controls were used for comparison ($n = 15$). At 4 months of age, 2 months post-transplantation, the VCN was determined in white blood cells by quantitative PCR (**Figure 2d,e**). Higher copy numbers were achieved with LV-CD11b than LV-PGK in the behavioral cohort: 1.2 versus 0.5 copies/cell, respectively, ($P < 0.001$) ($n = 8–12$) (**Figure 2d**) and in the biochemistry and histology cohort: 1.3 and 0.5 copies/cell ($n = 5$) ($P < 0.001$) (**Figure 2e**). At 6 months of age, 91–92% donor peripheral blood chimerism was achieved for LV-CD11b and LV-PGK, respectively, with no significant difference between them (**Figure 2f**). At 8 months of age, mice were killed, bone marrow was isolated from WT, LV-CD11b, and LV-PGK groups and the CFUs were assessed using methylcellulose culture ($n = 3$). There was neither significant difference in the total number of CFUs (**Supplementary Figure S2d**) nor in the percentage of CFUs of different lineages (**Supplementary Figure S2c**).

### LV-CD11b, but not LV-PGK, corrects open-field behavior of MPSIIIA mice

At 6 months of age, the 1-hour open-field test was performed to determine the effect of treatment on behavior[27]

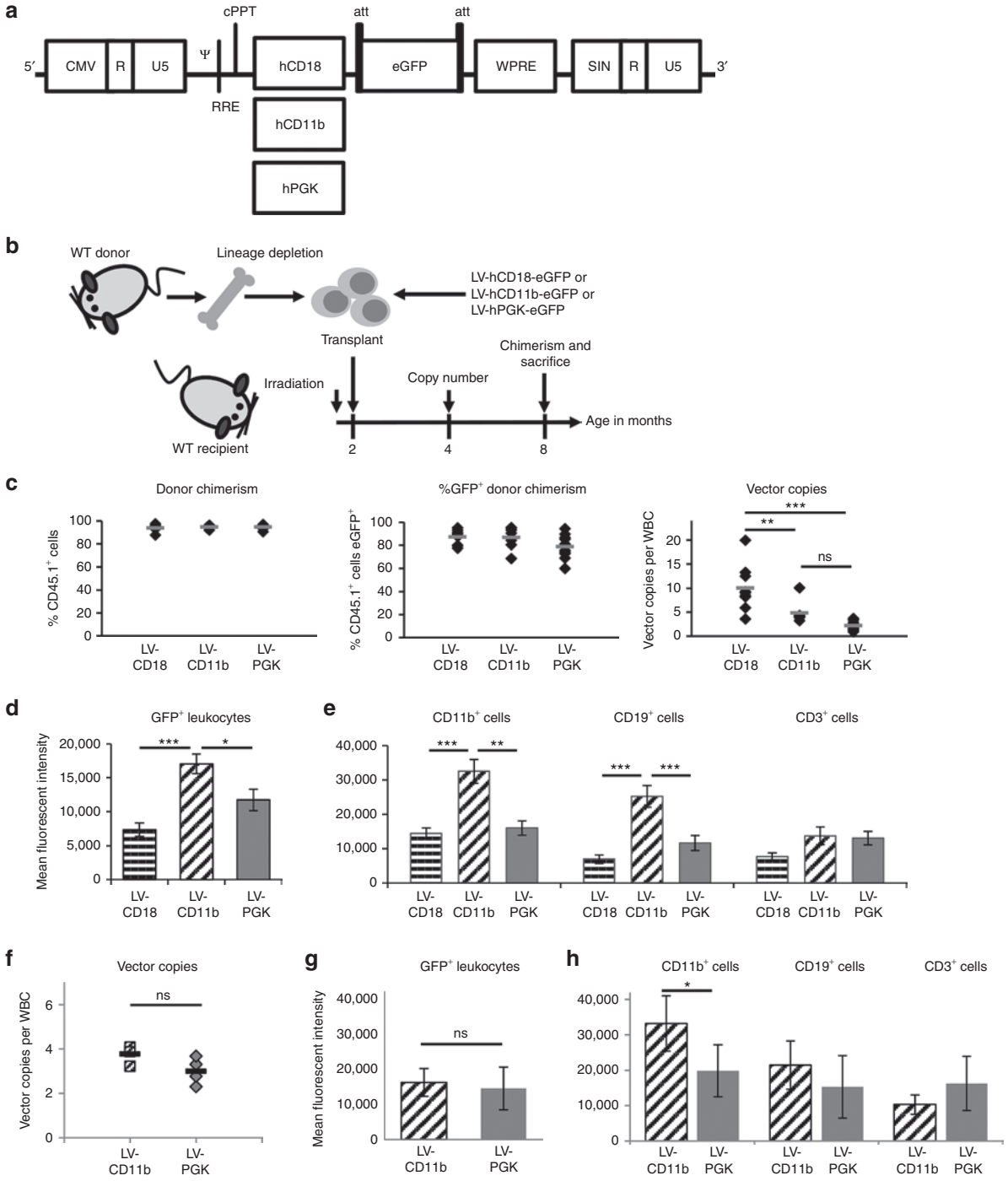


**Figure 1 Comparison of eGFP expression from myeloid promoters.** (**a**) pCCL LVs containing human CD18, CD11b, and PGK promoters driving eGFP expression. (**b**) WT bone marrow was lineage depleted and the enriched stem cell population transduced with LV-hCD18-eGFP, LV-hCD11b-eGFP, or LV-hPGK-eGFP at an MOI of 40–70 and transplanted into myeloablated WT mice. $n = 8–10$ (**c**) Donor and eGFP$^+$ chimerism was determined 24 weeks post-transplantation. The vector copy number (VCN) was determined in WBCs. (**d**–**e**) Mean fluorescent intensity of eGFP expression was determined for all leukocytes and for CD11b$^+$, CD19$^+$, and CD3$^+$ cells 24 weeks post-transplantation. (**f**–**h**) Mice with most equivalent copy numbers (VCN of 2.3–4.1) in WBCs were further compared. Error bars represent the SEM. Significant differences between the two groups marked with a line are demonstrated with $^*P < 0.05$; $^{**}P < 0.01$; and $^{***}P < 0.001$. CMV, cytomegalovirus; eGFP, enhanced green fluorescent protein; hPGK, human phosphoglycerate kinase; LV, lentiviral vector; MOI, multiplicity of infection; ns, nonsignificant; WBC, white blood cell; WT, wild-type.

(Figure 2g–j; **Supplementary Video S1** and **Supplementary Figure S2e,f**). MPSIIIA mice were hyperactive with significantly increased path length ($P = 0.002$) (Figure 2g), increased frequency ($P = 7.3 \times 10^{-5}$) (Figure 2i), and with a duration of motion over 100 mm/second ($P = 0.002$) (Figure 2j). MPSIIIA mice also have a reduced sense of danger, shown by significantly increased frequency of entries into the centre of the open field ($P = 0.022$) (Figure 2h).

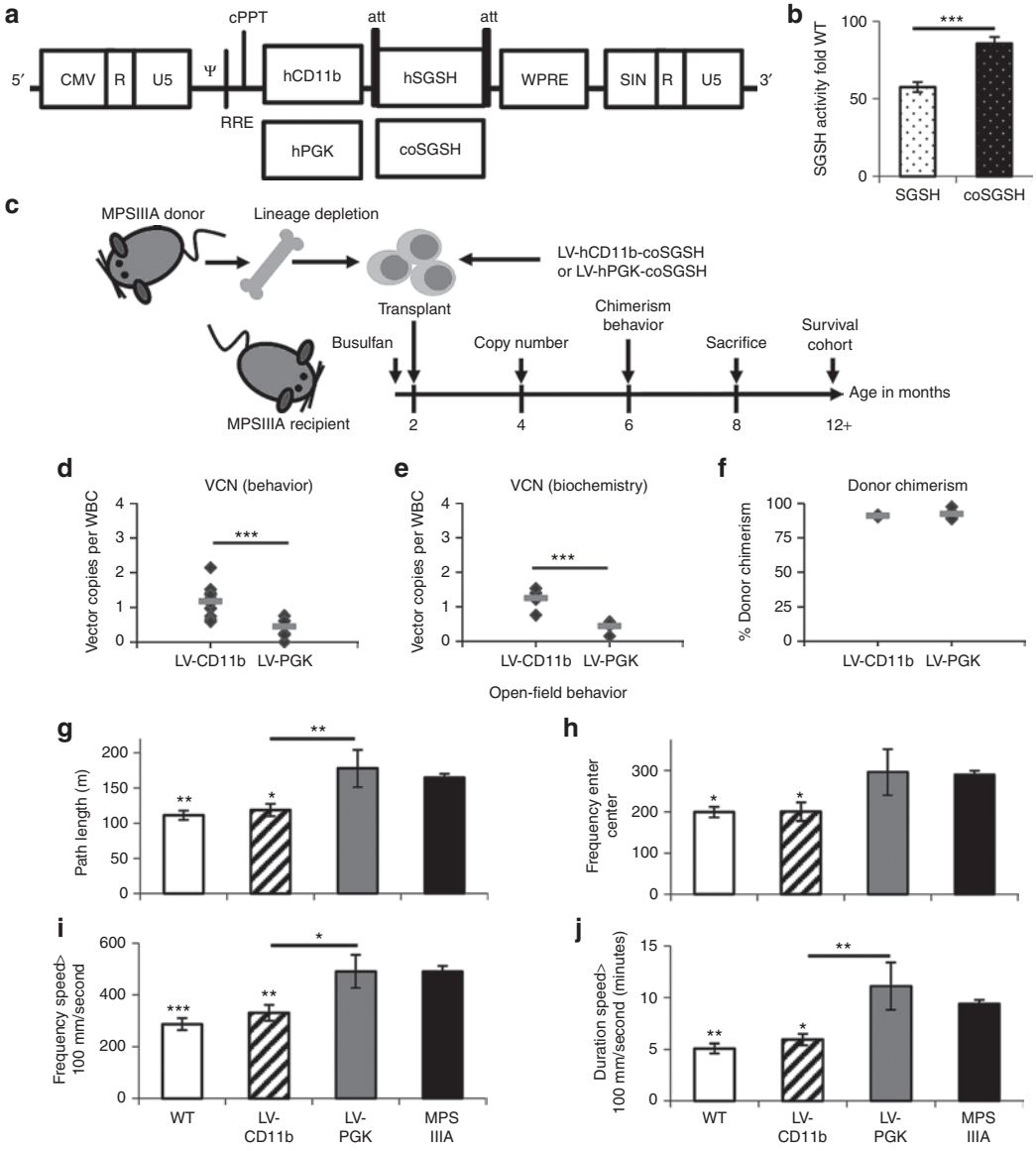


**Figure 2 LV-CD11b–modified autologous hematopoietic stem cells correct MPSIIIA mouse behavior.** (**a**) pCCL LVs were made containing either human CD11b or hPGK promoters driving normal or coSGSH. (**b**) Expression of hSGSH and coSGSH was compared by transient transfection of the human CHME3 microglial cell line. (**c**) MPSIIIA bone marrow was lineage depleted and transduced with LV-hCD11b-coSGSH or LV-hPGK-coSGSH at an MOI of 80, then transplanted into busulfan myeloablated MPSIIIA mice. (**d**,**e**) VCN was determined in WBCs (behavior $n$ = 8–12; biochemistry $n$ = 5). (**f**) 4 months post-transplantation, the donor chimerism in WBCs was determined by flow cytometry ($n$ = 3–7). (**g**–**j**) Open-field behavior was evaluated at 6 months (24 weeks) of age ($n$ = 8–15 female mice per group). The measures of hyperactivity were: (**g**) path length, (**i**) frequency, and (**j**) duration spent moving over 100 mm/second, while (**h**) frequency of centre entries measures thigmotaxis and may be a measure of sense of danger. Error bars represent the SEM. Significant differences to MPSIIIA, between the two groups marked with a line, are demonstrated with $^{*}P < 0.05$; $^{**}P < 0.01$; and $^{***}P < 0.001$. CMV, cytomegalovirus; coSGSH, codon-optimized human N-sulfoglucosamine sulfohydrolase; hPGK, human phosphoglycerate kinase; hSGSH, human N-sulfoglucosamine sulfohydrolase; LV, lentiviral vector; MOI, multiplicity of infection; MPSIIIA, mucopolysaccharidosis type IIIA; VCN, vector copy number; WBC, white blood cell; WT, wild-type.

LV-PGK had no significant effect on MPSIIIA behavior. In contrast, LV-CD11b fully normalized hyperactive behavior to WT levels with significant differences to MPSIIIA in all measures: path length ($P$ = 0.016) (Figure 2g), frequency ($P$ = 0.004) (Figure 2i), duration of motion over 100 mm/second ($P$ = 0.025) (Figure 2j), and frequency of centre entries ($P$ = 0.037) (Figure 2h). LV-CD11b was significantly better than LV-PGK in path length ($P$ = 0.007) (Figure 2g), frequency ($P$ = 0.015) (Figure 2i), and duration of motion over 100 mm/second ($P$ = 0.002) (Figure 2j) but not in centre entries.

## LV-CD11b improves brain-specific SGSH activity over LV-PGK and corrects primary HS storage of MPSIIIA mice

At 8 months of age, SGSH enzymatic activity was measured in perfused mice. LV-CD11b and LV-PGK significantly increased SGSH activity to 472% of WT ($P = 5.1 \times 10^{-12}$) and 576% ($P = 3.5 \times 10^{-12}$), respectively, in bone marrow (Figure 3a) and to 162% of WT ($P = 2.4 \times 10^{-11}$) and 245% ($P = 6.0 \times 10^{-12}$), respectively, in the spleen (Figure 3b). In the liver (Figure 3c), LV-CD11b and

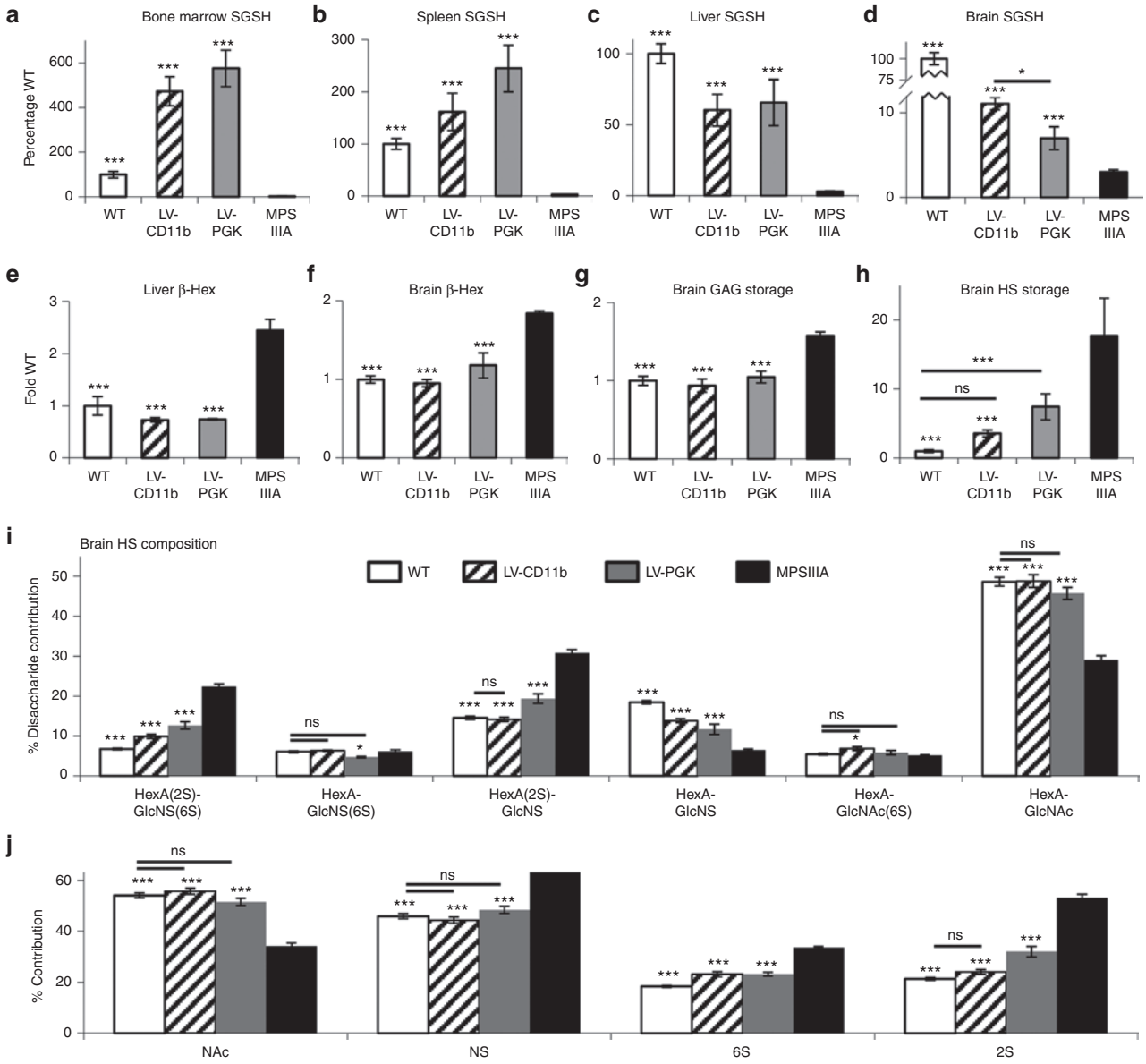


**Figure 3 LV-CD11b improves brain-specific SGSH activity over LV-PGK and corrects primary HS storage of MPSIIIA mice.** At 8 months of age, SGSH enzyme activity was measured in (**a**) bone marrow, (**b**) spleen, (**c**) liver, and (**d**) brain of perfused mice ($n = 5$). Secondary upregulation of β-Hex was measured in (**e**) liver and (**f**) brain. (**g**) Total sulfated GAG in the brain was measured with the dye binding Blyscan assay. (**h**) Total HS storage was measured by 2-aminoacridone (AMAC)–labeled disaccharide analysis. The different HS disaccharides were quantified by (**i**) AMAC, and (**j**) the relative proportion of HS that was NAc, NS, 6S, and 2S was also determined. Error bars represent the SEM. Significant differences to MPSIIIA are marked with $^{*}P < 0.05$ and $^{***}P < 0.001$. Treatments that are not significantly different to WT are marked with a line and ns (nonsignificant) ($P > 0.05$). 6S, 6-*O*-sulfated; 2S, 2-*O*-sulfated; β-Hex, β-N-acetyl hexosaminidase; GAG, glycosaminoglycan; HS, heparan sulfate; LV, lentiviral vector; MPSIIIA, mucopolysaccharidosis type IIIA; NAc, *N*-acetylated; NS, *N*-sulfated; PGK, phosphoglycerate kinase; SGSH, N-sulfoglucosamine sulfohydrolase; WT, wild-type.

LV-PGK significantly increased SGSH activity to 60% of WT ($P = 6.5 \times 10^{-9}$) and 66% ($P = 5.7 \times 10^{-9}$), respectively. In the peripheral organs, there was no significant difference in SGSH activity between LV-CD11b and LV-PGK. However, in the brain (**Figure 3d**), LV-CD11b significantly increased SGSH activity to 11% of WT ($P = 2.2 \times 10^{-6}$), which was significantly higher than LV-PGK ($P = 0.024$), at 7% of WT ($P = 7.3 \times 10^{-4}$).

Increased lysosomal compartment size results in upregulation of other lysosomal enzymes by the transcription factor EB,[28] therefore, β-N-acetyl hexosaminidase (β-Hex) activity was also measured in liver (**Figure 3e**) and brain (**Figure 3f**). Both LV-CD11b and LV-PGK significantly reduced β-Hex activity to normal levels (liver $P = 9.8 \times 10^{-7}$, $P = 1.0 \times 10^{-6}$, respectively; brain $P = 2.1 \times 10^{-5}$, $P = 6.6 \times 10^{-4}$, respectively).

Total glycosaminoglycan (GAG) measured by Blyscan was 1.6-fold elevated in MPSIIIA brain and significantly reduced by both the treatments (**Figure 3g**). Total HS determined by 2-aminoacridone–labeled disaccharide analysis was 18-fold elevated in MPSIIIA mouse brains (**Figure 3h**). LV-CD11b significantly corrected HS in the brain ($P = 0.003$) to a level where it was no

longer significantly different from WT. LV-PGK did not significantly reduce HS ($P$ = 0.057), remaining significantly elevated over WT ($P$ = 0.001). HS sulfation has an important functional role, thus HS disaccharides were quantified (**Figure 3i**). There was a significant increase in highly sulfated HexA(2S)-GlcNS(6S) and HexA(2S)-GlcNS ($P = 1.4\times10^{-10}$ and $P = 3.6\times10^{-9}$, respectively) and a commensurate reduction in HexA-GlcNS and HexA-GlcNAc ($P = 5.6\times10^{-8}$ and $P = 1.1\times10^{-7}$, respectively) between WT and MPSIIIA. There was no significant difference between WT and MPSIIIA in HexA-GlcNS(6S) or HexA-GlcNAc(6S) HS disaccharides. LV-CD11b normalized HexA(2S)-GlcNS and HexA-GlcNAc and significantly corrected HexA(2S)-GlcNS(6S) and HexA-GlcNS. LV-PGK also improved the four abnormal HS disaccharides but only corrected HexA-GlcNAc.

Overall, HS from MPSIIIA mouse brain is significantly *N*-sulfated ($P = 2.7\times10^{-8}$), 6-*O*-sulfated (6S) ($P = 2.1\times10^{-10}$), and 2-*O*-sulfated (2S) ($P = 2.4\times10^{-10}$) with a commensurate reduction in un-sulfated *N*-acetylated (NAc) ($P = 3.4\times10^{-8}$) HS (**Figure 3j**). LV-CD11b normalized NAc, *N*-sulfated, and 2S HS to WT levels and significantly corrected 6S ($P = 9.5\times10^{-8}$) HS. LV-PGK corrected NAc and *N*-sulfated HS, but was only able to reduce 2S ($P = 7.1\times10^{-8}$) and 6S ($P = 4.5\times10^{-8}$) HS.

## LV-CD11b normalizes the neuronal lysosomal compartment and most areas of neuroinflammation, while both LV-CD11b and LV-PGK mediate improvements in secondary brain markers in MPSIIIA mice

To determine the effects of increased SGSH on the neuronal lysosomal compartment, the lysosomal stain LAMP2 (green) was colocalized with neuronal cells using NeuN (red) (**Figure 4**). In MPSIIIA NeuN-positive cells, there was intense coregistered cytoplasmic staining of lysosomes, whereas in WT mice, LAMP2 staining was weaker, punctuate, and perinuclear. LV-CD11b appeared to correct this to WT levels and LV-PGK also mediated correction of the majority of this in the cerebral cortex (**Figure 4a**). We also characterized the medial nucleus region of the amygdala as we previously found this region of the brain to be less well corrected by gene therapy than the cerebral cortex[3] and it is involved in processing memory, emotional responses, and behavior.[29] The lysosomal compartment was also intensely stained in MPSIIIA compared with WT mice and a significant proportion of staining was in NeuN-negative cells, although this could reflect slightly lower neuronal density. In the amygdala and the rest of the brain, the lysosomal compartment appeared normal in LV-CD11b–treated mice (**Figure 4b**), whereas LV-PGK had less effect in correcting abnormal LAMP2 staining than LV-CD11b.

Severe neuroinflammation is present throughout the MPSIIIA brain[4,9] (**Supplementary Figure S3**). There were 8.9-fold more isolectin B4 (ILB4)-positive microglia than normal in MPSIIIA cerebral cortex (**Figure 5a**). LV-CD11b normalized microglial numbers to WT levels in cortex ($P = 2.7\times10^{-7}$), while LV-PGK reduced them from MPSIIIA ($P = 2.0\times10^{-4}$) but was still significantly elevated above WT levels ($P$ = 0.004). A 64-fold increase in ILB4-positive microglia in MPSIIIA mice was observed in the medial nucleus region of the amygdala (**Figure 5b**). LV-CD11b corrected ($P$ = 0.0004) the number of microglia and LV-PGK

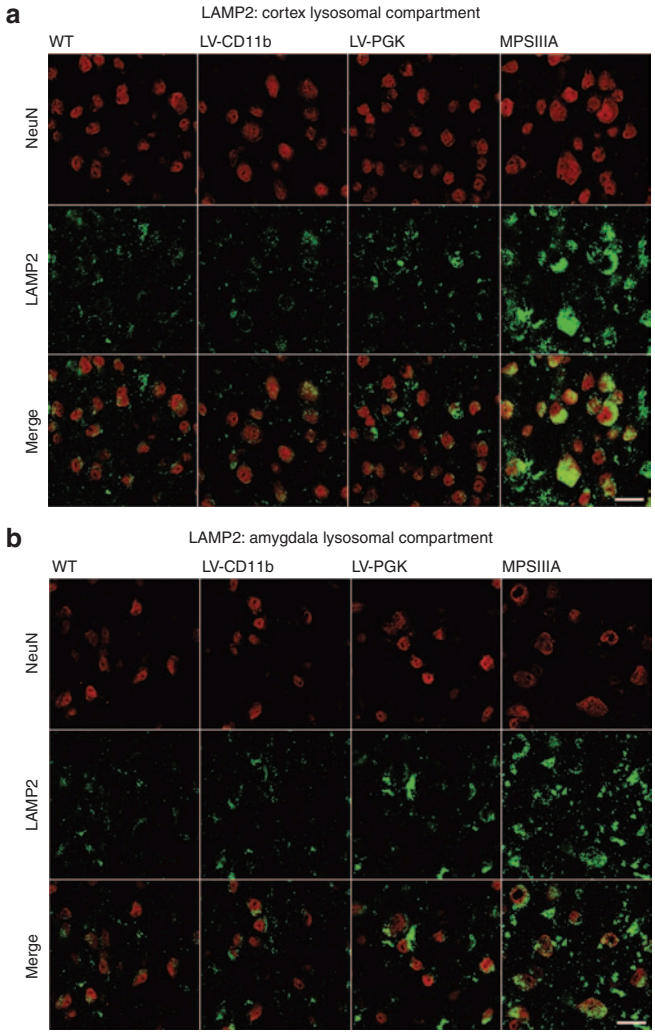


**Figure 4 LV-CD11b corrects lysosomal compartment size in MPSIIIA brains.** Representative confocal images of (**a**) brain cortex (layer IV/V) and (**b**) amygdala (medial nucleus) from approximately –1.18 mm relative to bregma were stained with LAMP2 for lysosomal compartment (green) and NeuN for neuronal nuclei (red), and representative images are shown. Bar = 20 µm. LV, lentiviral vector; MPSIIIA, mucopolysaccharidosis type IIIA; PGK, phosphoglycerate kinase; WT, wild-type.

reduced the number ($P = 9.5\times10^{-6}$) but these remained significantly elevated ($P$ = 0.007). Despite normalization by CD11b in these brain regions, elevated numbers of microglial cells remained in other brain regions including the globus pallidus, thalamus, and hypothalamus, although all were much improved over either PGK or MPSIIIA (**Supplementary Figure S3**). There were 25-fold more astrocytes than normal in MPSIIIA cerebral cortex (**Figure 5c**). LV-CD11b normalized astrocyte numbers in the cortex ($P = 1.9\times10^{-7}$), and mostly throughout the brain, whereas LV-PGK significantly reduced them from MPSIIIA ($P = 4.2\times10^{-4}$) but was still significantly elevated above WT ($P$ = 0.0018) and above LV-CD11b levels ($P$ = 0.018). A twofold increase in astrocytes in MPSIIIA mice was observed in amygdala (**Figure 5d**). LV-CD11b and LV-PGK both normalized astrocyte numbers.

MPSIIIA is also characterized by secondary storage of GM2 ganglioside in the brain, particularly in lamina II/III and V/VI

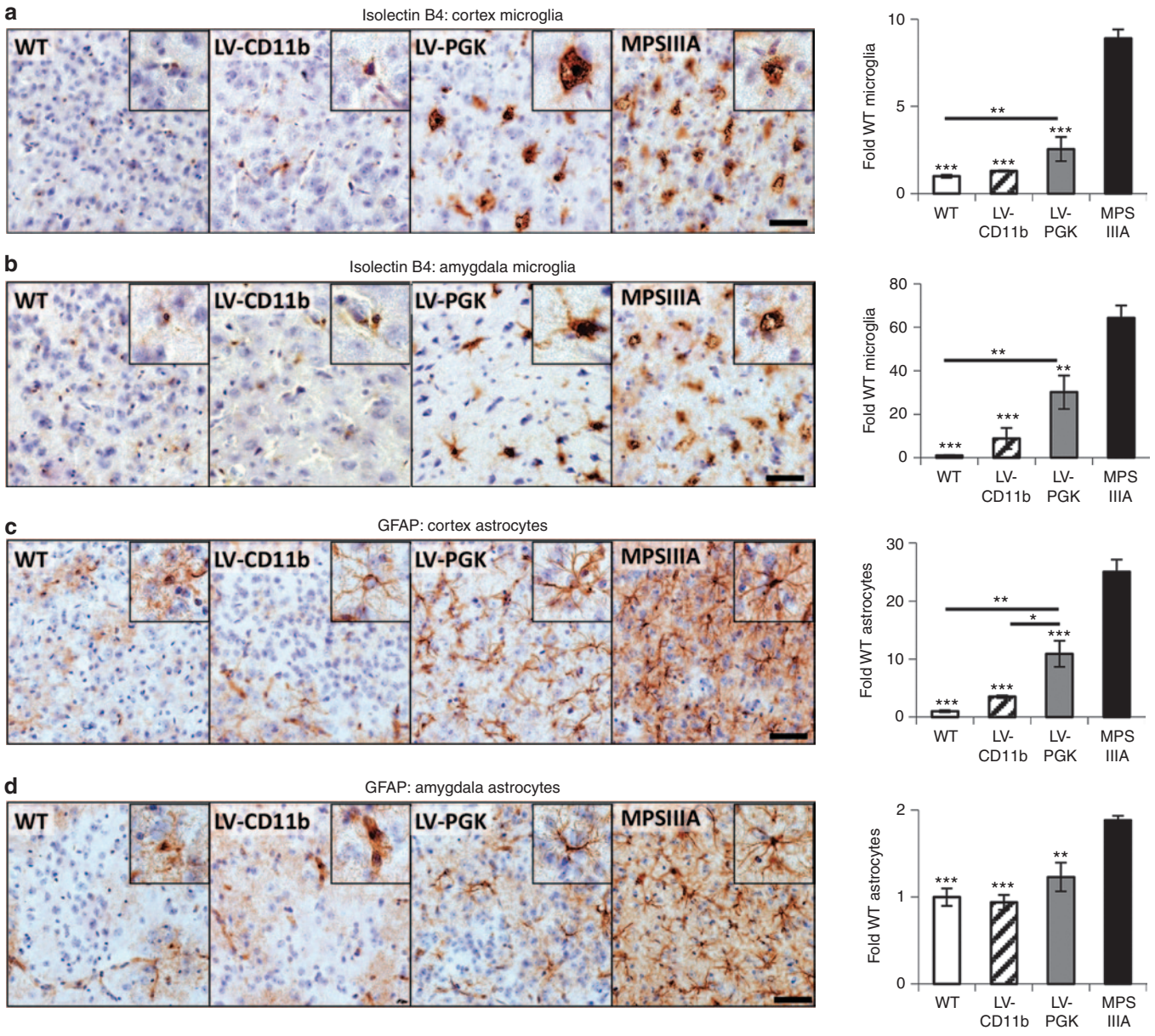


**Figure 5 LV-CD11b normalizes neuroinflammation in the cerebral cortex and amygdala of MPSIIIA mice, while LV-PGK mediates improvements in neuroinflammation.** Four brain sections per mouse ($n$ = 5 per group), taken from approximately bregma 0.26, –0.46, –1.18, and –1.94 mm, were stained and quantified with isolectin B4 for microglia number in the (**a**) cerebral cortex and (**b**) amygdala or with GFAP for astrocytes in the (**c**) cerebral cortex and (**d**) amygdala. Representative images from the cerebral cortex (layer IV/V) and the amygdala, both from approximately –1.18 mm relative to bregma, are shown. Sections were counterstained with Mayer's hematoxylin to highlight the nuclei (blue). Error bars represent the SEM. Significant differences to MPSIIIA, between the two groups marked with a line, are demonstrated with *$P$ < 0.05, **$P$ < 0.01; and ***$P$ < 0.001. Bar = 50 µm. LV, lentiviral vector; MPSIIIA, mucopolysaccharidosis type IIIA; PGK, phosphoglycerate kinase; WT, wild-type.

of the primary motor, somatosensory, and parietal areas of cerebral cortex and amygdala with no staining detected in WT mice (**Supplementary Figure S4**).[4] LV-CD11b and LV-PGK both ($P = 4.3 \times 10^{-8}$ and $P = 1.4 \times 10^{-7}$, respectively) corrected GM2 ganglioside storage in the cerebral cortex (**Figure 6a**). GM2 ganglioside storage was nearly sevenfold elevated in amygdala of MPSIIIA mice and was completely cleared by LV-CD11b (**Figure 6b**), but it was only reduced with LV-PGK. Again, despite normalization in these brain regions, LV-CD11b showed mild elevations of GM2 ganglioside staining in other brain regions including globus pallidus, thalamus, and retrosplenial granular cortex. LV-PGK showed more significant GM2 ganglioside staining in these regions, particularly in the amygdala, and untreated MPSIIIA were worse again (**Supplementary Figure S4**).

Presynaptic vesicle dysregulation has also been observed in the MPSIIIA brain *via* changes in VAMP2 from punctate vesicular staining to diffuse.[4] LV-CD11b and LV-PGK both significantly ($P = 1.4 \times 10^{-5}$ and $P = 8.0 \times 10^{-5}$, respectively) corrected VAMP2 localization in the cerebral cortex (**Figure 6c**). We observed no statistical differences in VAMP2 staining in amygdala (**Figure 6d**).

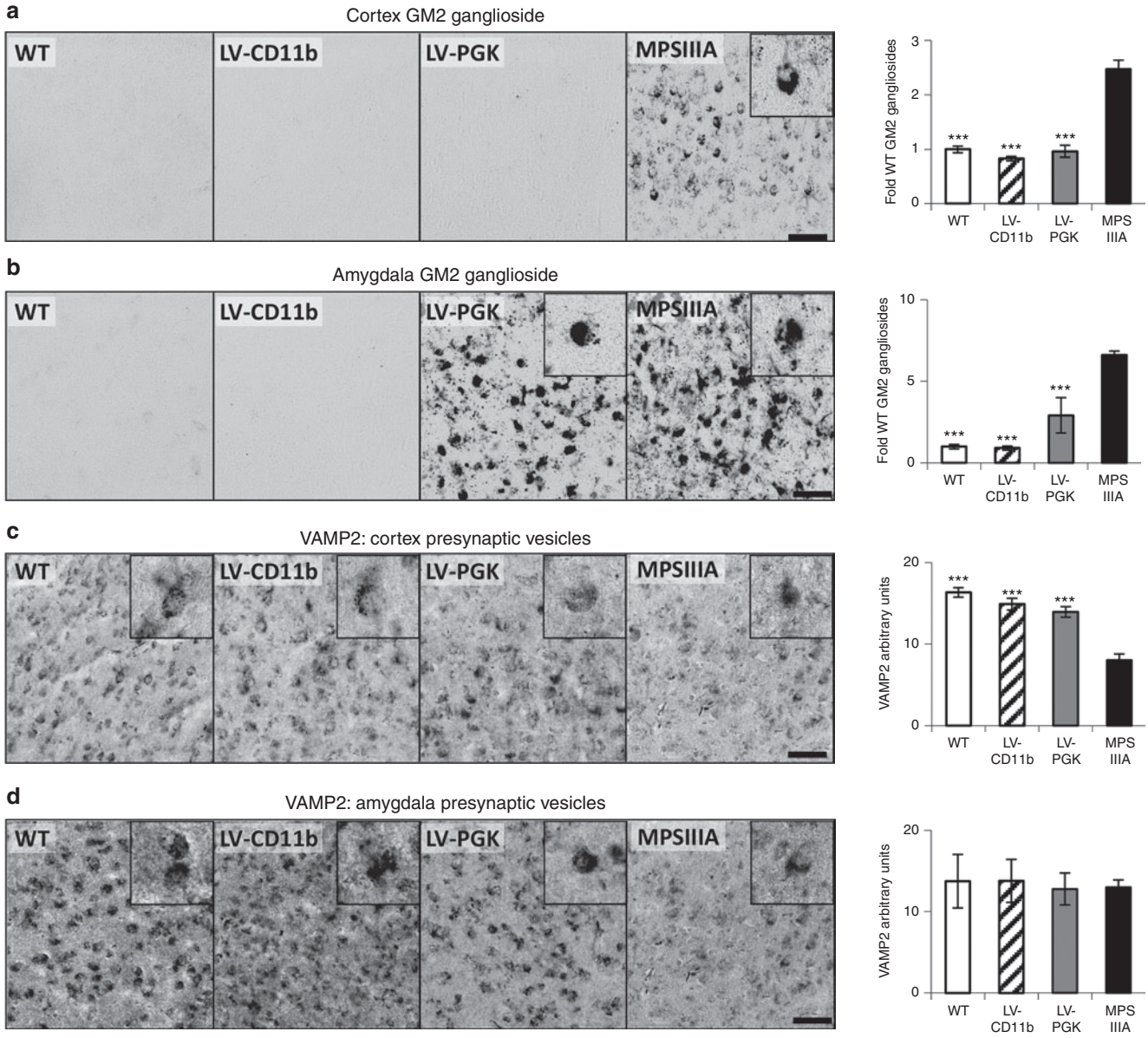


**Figure 6 LV-CD11b and LV-PGK both correct secondary storage and presynaptic vesicles in the cerebral cortex, while LV-PGK is less effective in the amygdala of MPSIIIA mice.** Four brain sections per mouse ($n = 5$ per group), taken from approximately bregma 0.14, –0.58, –1.3, and –2.06 mm, were stained and quantified for GM2 ganglioside in the (**a**) cerebral cortex and (**b**) amygdala, and VAMP2 for presynaptic vesicles in the (**c**) cerebral cortex and (**d**) amygdala. Representative images from the cerebral cortex (layer IV/V) and the amygdala, both from approximately –1.3 mm relative to bregma, are shown. Error bars represent the SEM. Significant differences to MPSIIIA, between the two groups marked with a line, are demonstrated with ***$P < 0.001$. Bar = 50 µm. LV, lentiviral vector; MPSIIIA, mucopolysaccharidosis type IIIA; PGK, phosphoglycerate kinase; WT, wild-type.

## DISCUSSION

This study demonstrates neurological and open-field behavioral correction of the mouse model of MPSIIIA using a clinically relevant therapeutic approach. The CD11b promoter enhanced eGFP expression in CD11b$^+$ and CD19$^+$ cells in contrast to CD18, which was more specific but less effective than PGK or CD11b. Both myeloid promoters were previously evaluated in retroviral vectors with poor expression in cell lines compared with ubiquitous promoters.[30] We also found myeloid promoters to be ineffectual in monocyte/macrophage cell lines, and it was only in hematopoietic cells *in vivo* that CD11b expression was high. We achieved slightly higher copy numbers from CD11b vectors than PGK vectors, however, by comparing CD11b-eGFP and PGK-eGFP mice with similar copy numbers (average: 3.77, 3.01 respectively; nonsignificant), we found that CD11b promoter yielded 67% significantly higher expression in CD11b$^+$ cells (33,199 versus 19,846; $P < 0.05$), with no significant differences in other lineages (**Figure 1f–h**).

The LV-CD11b vector mediated significant improvements in SGSH expression with 11% of WT activity in the entire brain *via* monocyte/microglial-enhanced expression in brain engrafted cells compared with 7% using the ubiquitous PGK promoter. The

difference was sufficient to mediate correction of hyperactive behavior in LV-CD11b–treated mice with no change in LV-PGK–treated mice. Analysis of SGSH brain enzyme levels across all treated MPSIIIA mice[3] allowed us to determine the minimal effective brain enzyme level mediating behavioral normalization, to be ~8.5% of normal enzyme activity (data not shown).

We achieve a similar level of brain SGSH activity to that reported after intravenous adeno-associated virus serotype-9 expressing SGSH in MPSIIIA mice (6–12%).[11] In this paper, activity was lower in female mouse brains (6–8%), at levels we would predict to be subtherapeutic, while behavior was not evaluated. In addition, 8–17% activity was reported following direct brain injection of adeno-associated virus serotype-2/5 expressing SGSH/SUMF1 in MPSIIIA mice[10] but injection site-localized substrate correction was reported in this case. The efficacy of both approaches could be reduced on scale-up due to reliance on vector correction of brain cells and because enzyme is not reported to cross the blood–brain barrier in significant quantity.[31] In contrast, donor microglia are distributed throughout the brain following autologous LV-HSC gene therapy, and clinical experience in immunodeficiencies[32] suggests that mouse–human scale-up is not problematic. The GAG dye binding assay gives a misleading indication of correction by LV-PGK in the brain (**Figure 3g**), whereas the 2-aminoacridone assay measuring HS *via* high-performance liquid chromatography is much more sensitive and showed that LV-PGK had reduced excess HS, but not significantly to WT levels (**Figure 3h**). Although the GAG assay is commonly used, preclinical demonstrations of neurological correction in MPS diseases should rely on measurements of brain HS in the context of several other markers as well as demonstrable behavioral correction.

Neuroinflammation in terms of microglial and astrocyte cell numbers was almost completely corrected by LV-CD11b in both the cortex and amygdala, and significantly improved throughout the brain in contrast to our previous findings.[3] Neuroinflammation was only partially corrected by LV-PGK. Amygdala was studied because we had previously observed incomplete correction of secondary pathology and neuroinflammation in this region.[3] Notably, in MPSIIIA, the amygdala has significantly increased microglial activation over cortex (64-fold versus ninefold), with comparatively lower astrocytosis (twofold versus 25-fold). Neuroinflammation is very much a global phenomenon in the MPSIIIA mouse brain, thus it is intriguing that certain brain regions retain some inflammation in the LV-CD11b mice (**Supplementary Figure S3**), despite behavioral correction. This may reflect the distance of less well corrected areas such as the globus pallidus and thalamus from ventricular spaces, which we presume are the major routes of delivery for donor monocytes into the brain resulting in lower distribution of donor cells in these areas.

Secondary storage of GM2 ganglioside was corrected by LV-CD11b in cerebral cortex, amygdala, and in most regions of the brain and by LV-PGK in the cortex, but staining remained in the LV-PGK–treated amygdala and in several other brain regions, in line with our previous observations.[3] The correction of open-field behavior by LV-CD11b but not by LV-PGK could be related to the residual staining observed in the amygdala in LV-PGK–treated mice for both LAMP2 and GM2 ganglioside staining as the amygdala has a role in memory, processing emotions, and behavioral reactions[29] and is postulated to play a role in the behavior of MPSIIIA patients. In support of this, we observed small elevations of GM2 ganglioside staining in the thalamus, retrosplenial granular cortex, and the hypothalamus, but not in the amygdala of LV-CD11b–treated mice. However, we also observed neuroinflammatory differences between LV-CD11b and LV-PGK in both cerebral cortex and amygdala; moreover, in a previous study, where behavioral correction was observed, GM2 ganglioside storage was still present in the amygdala, which suggests that GM2 ganglioside storage in this region is not the primary cause of pathology.[3] In our previous study, we observed behavioral correction with only partially corrected neuroinflammation, thus we would hypothesize that differences in primary storage of HS and lysosomal function may be more important in determining behavioral changes. Although HS has a role in stimulating inflammation *via* Toll-like receptor 4, ablation of Toll-like receptor 4 or downstream MyD88 signaling in the similar mouse model of MPSIIIB delayed neuroinflammation, but not the appearance of other markers of neurodegeneration.[33] HS, GM2 and GM3 gangliosides could instead act as danger-associated molecular patterns, exacerbating inflammation *via* both Toll-like receptor-mediated and antigen-driven adaptive immune responses.[34,35] Although we know that excess HS is present outside cells in plasma and urine of patients with MPS diseases,[36–39] critical to the implication of HS in Sanfilippo disease pathology would be the identification of a functional role for the primary HS storage material in neuropathology.

Overall, LV-CD11b corrected many pathological markers to, or near to, WT levels in most areas of the brain. In contrast, LV-PGK had lower brain enzyme expression, which resulted in sustained elevation of pathological markers in many brain areas. Open-field behavior was much more biphasic, and this may reflect a functional threshold effect at the cellular level, where clearance of pathological markers to a certain level resolves function, rather than specific brain areas being responsible for neuropathology.

Of note, the normalization in the number of activated microglia in the cortex and amygdala by LV-CD11b did not impact on enzyme delivery. Although this study was not setup to answer this question, donor microglial repopulation could be independent of microgliosis. Busulfan conditioning results in 22% donor-derived $Iba1^+$ microglial repopulation of the brain or 30% $CD11b^+CD45^{lo}$ donor-derived mcroglia,[40,41] but donor cells may not be responsible for microgliosis. There is also a potential contribution from $CD11b^+$ neutrophils to brain enzyme activity as these are also known to traffic into the brain.

Most studies evaluating autologous LV-HSC gene therapy have utilized ubiquitous promoters. The PGK promoter was used in MPSI mice to drive expression of IDUA and resulted in 100-fold overexpression of IDUA activity in peripheral blood mononuclear cells. This was achieved with copy numbers of 11 per cell.[21] Although overexpression of IDUA was not shown to be toxic, it could impact on other gene products. In MPSI, higher than normal levels of IDUA may be beneficial in treating the skeletal manifestations, but in primarily neurological disorders, enhancing expression in the brain while limiting peripheral overexpression is a prudent safety approach. Indeed, in the mouse model of Krabbe disease, GALC expression was found to be toxic to HSCs and progenitors,

forcing a micro RNA-regulated approach to therapy.[42] In this study, we achieved significantly higher enzyme levels in the brain with the CD11b promoter compared with PGK and similar enzyme levels in the periphery with both promoters (5-fold over normal). Notably, LV-CD11b–mediated neurological correction was achieved with clinically relevant copy numbers per cell of 1.2. We had higher copy numbers in CD11b- versus PGK-treated MPSIIIA mice, but increased PGK copy number would have also resulted in increased peripheral overexpression between tenfold and 15-fold of normal, and was not achievable in our hands with this promoter. Although peripheral overexpression may not be an issue with SGSH or IDUA, wider application of this approach as a neurological disease treatment makes the targeted myeloid-specific approach a safer and more specific alternative. Neurological correction of the mouse model of metachromatic leukodystrophy was achieved with only 10% brain enzyme and this and other work has resulted in subsequent clinical trials.[22,23] On the basis of these and our own demonstration of preclinical efficacy, we propose a myeloid driven autologous HSC gene therapy approach to treat MPSIIIA patients.

## MATERIALS AND METHODS

***Mice.*** *In vivo* procedures were ethically approved under UK Home Office regulations and PPL 40/3117. MPSIIIA mice[7] on a C57BL/6J background (B6.Cg-Sgsh$^{mps3a}$/6J) were maintained by heterozygote breeding.[3,4,27] MPSIIIA backcrossed to PEP3 CD45.1 (B6.SJL-*Ptprc*$^{a}$ *Pepc*$^{b}$/BoyJ) were used to distinguish donor and recipient cells as previously described.[3] WT littermate controls were used throughout.

***Construction of LVs.*** The SGSH gene flanked with Att B1/2 sites was inserted into *Bam*HI/*Sal*I restriction sites in the third-generation LV #277 pCCLsin.cPPT.hPGK.eGFP.Wpre[22] in place of eGFP. Human CD11b and CD18 promoters were amplified from human gDNA from peripheral blood. Primers were based on sequences from GenBank: M77675.1 for the CD18 promoter and M84477 for the CD11b promoter[25,26] – CD11b forward 5′-CTCGAGGATATC ATTTTTTTGTAGAGACAGGGTCTCT-3′; CD11b Rev 5′-GGATCC GGCTGGAAGGAGCCAGAA-3′; CD18 forward 5′-CTCGAGGATATC TGGCCTCTGTGTTCTTCTTC-3′, CD18 Rev 5′-GGATCC CCTCGGTGTGCTGGAGTC-3′. Promoters were exchanged with PGK in the LV backbone at *Xho*I and *Bam*HI sites.

SGSH was codon optimized by Life Technologies (Paisley, UK), and cloned into LV-PGK and LV-CD11b using Gateway cloning (Life Technologies).

The start codon and promoter of WPRE X protein were mutated to the mut6 configuration[43] by exchange of the SalI/SacII fragment from pHR. SFFV.SGSH.[3]

***LV production and titration.*** The LV was produced as previously described by transient transfection of HEK 293T cells with pMD2G, pΔ8.91gag/pol, and the LV plasmid.[3,44,45] LV was titered using quantitative PCR.[3] EL4 mouse lymphoma cells (ATCC no. TIB-39; ATCC, Manassas, VA) were transduced with three dilutions of concentrated LV and collected 72 hours later. DNA was extracted using GenElute Mammalian Genomic DNA Miniprep kit (Sigma-Aldrich, Poole, UK) and the number of integrated viral genomes per cell was determined using quantitative PCR as follows. The TaqMan universal PCR master mix (Applied Biosystems, by Life Technologies, Paisley, UK) was added with glyceraldehyde 3-phosphate dehydrogenase forward (5′-TGCACCACCAACTGCTTAGC-3′) and reverse (5′-AGAACATCATCCCTGCATCC-3′) primers and a VIC probe (Applied Biosystems), and WPRE forward (5′-CCGTTGTCAGGCAACGTG-3′) and reverse (5′-AGCTGACAGGTGGTGGCAAT-3′) primers and FAM/TAMRA probe (5′-TGCTGACGCAACCCCCACTGGT-3′), and a DNA template (1 ng). Each sample was run in duplicate. The PCR reaction was performed using an ABI PRISM 7700 Sequence detector (Applied Biosystems) at the settings: 50 °C for 2 minutes, 95 °C for 10 minutes, followed by 40 cycles for 15 seconds, and 60 °C for 1 minute. The data were analyzed using sequence Detection System version 1.9.1 software (Applied Biosystems). The number of integrations was determined using a standard curve generated by serial dilutions of DNA sample derived from an EL4 cell line clone (ALS EL4 eGFP 2.2) containing two copies of integrated WPRE gene/cell. The VCN in the range of 0.1–5 integrations/cell was used to calculate the titer.

***Mouse HSC transduction and transplantation.*** Performed as previously described.[3,44,45] Briefly, myeloablative conditioning was two 5 Gy irradiation separated by 4 hours (eGFP) or 125 mg/kg Busulfan (Busilvex; Pierre Fabre, Boulogne, France) intraperitoneal over 5 days (MPSIIIA). Mouse bone marrow was isolated, lineage depleted (Stem Cell Technologies, Grenoble, France), and incubated at 37 °C 5% $CO_2$ in X-Vivo-10 (Lonza, Slough, UK), 2% bovine serum albumin (Sigma-Aldrich), 100 ng/ml murine SCF (R&D Systems, Abingdon, UK), 100 ng/ml mFlt3-Ligand (R&D System), and 10 ng/ml mIL-6 (R&D Systems) for 3 hours before lentiviral transduction.

***VCN determination.*** VCN was determined from white blood cells using quantitative PCR as previously described.[3]

***Sample processing.*** At 8 months of age, mice were anesthetized and transcardially perfused with 37 °C Tyrode's solution to remove blood from organs as previously described.[3] Pieces of liver and spleen and one hemisphere of brain were frozen at −80 °C. The other brain hemisphere was fixed in 4% paraformaldehyde for 24 hours, then 30% sucrose 2 mmol/l $MgCl_2$/phosphate-buffered saline for 48 hours before freezing at −80 °C. For SGSH and HS assays, samples were homogenized and sonicated in homogenization buffer (0.5 mol/l NaCl, 0.02 mol/l Tris pH 7–7.5), then centrifuged at 2,200*g* for 15 minutes at 4 °C, and the supernatant was collected. Protein concentration was determined using Pierce BCA assay kit (Fisher Scientific, Loughborough, UK) assay according to manufacturer's instructions.

***SGSH enzymatic activity.*** SGSH enzymatic activity was quantified as previously described.[3] Tissue samples were homogenized and sonicated to extract protein, which was measured using Pierce BCA assay kit (Fisher Scientific); 60 µg of brain protein, 40 µg of liver, 40 µg of spleen, and 16 µg of bone marrow protein were analyzed. The assay was performed as per manufacturer's instructions (Moscerdam Substrates, Oegstgeest, the Netherlands) with minor modifications. Samples were first incubated for 17 hours at 42 °C with SGSH substrate 4-methylumbelliferyl-α-D-sulfoglucosamine (4-MU-αGlcNS; Moscerdam Substrates), followed by 24 hours at 37 °C with α-glucosidase enzyme, which resulted in release of 4-methylumbelliferone fluorescent substance. Fluorescence was measured at excitation 360 nm and emission 460 nm using a Synergy HT Microplate reader (BioTec, Potton, UK).

***Blyscan assay for total GAGs.*** The Blyscan assay for total sulfated GAGs was performed as previously described, except 350 µg of protein was used.[3]

***CFU assay.*** At 8 months of age, 6 months post-transplantation, bone marrow was isolated from WT, LV-CD11b, and LV-PGK mice and set up in MethoCult culture (Stem Cell Technologies) as previously described[3,45] to assess CFU lineage development.

***Open-field behavior.*** Performed as previously described.[3,27,46,47] Each mouse was tested at 6 months of age 1.5 hours into the 12-hour light phase to ensure the same circadian time point. Mice were dropped into the centre of an open-field arena (width 450 mm, depth 450 mm, height 500 mm) made of matt white acrylic; and behavior was recorded for 1 hour using a digital camcorder (Sony, Weybridge, UK). The data were analyzed using TopScan suite software version 2.0 (Clever Sys, Reston, VA). The total path length, frequency and duration of rapid exploratory behavior (speed

>100 mm/s), duration of immobility (speed <5 mm/s), and frequency of entering the centre and duration in the centre (75 mm from each edge) were analyzed.

***2-aminoacridone–labeled disaccharide analysis of HS.*** Analysis of the quantity and sulfation state of HS using 2-aminoacridone labeling and high-performance liquid chromatography was determined as previously described.[2]

***Immunohistochemistry.*** Four brain sections per mouse taken from, approximately, bregma 0.26, −0.46, −1.18, and −1.94 mm were stained and quantified by counting ILB4- or GFAP-positive cells or by measuring stain intensity for GM2 gangliosides and VAMP2 as previously described.[4,47,48] LAMP2 staining was performed on sections from approximately −1.18 mm relative to bregma as previously described.[3]

***Immunohistochemical staining for GFP, NeuN, and LAMP2.*** Sections were blocked in 5% goat serum, 1 mg/ml bovine serum albumin, and 0.1% Triton X-100 in Tris-buffered saline (TBS) for 1 hour, then incubated overnight at 4 °C with chicken anti-GFP antibody (1:1,000; Abcam, Cambridge, UK) or both mouse anti-NeuN IgG (1:100; Millipore, Watford, UK) and rat anti-LAMP2 IgG (0.25 µg/ml; developed by August, J, Developmental Studies Hybridoma Bank, University of Iowa, Iowa City, IA) in blocking solution, washed in TBS, and stained with Alexa 488 goat anti-chicken IgG for the GFP primary antibody (1:1,000; Life Technologies) or both Alexa 488 goat anti-mouse and Alexa 594 goat anti-rat IgG (1:1,000; Life Technologies) in blocking solution for 1 hour in the dark. After washing with TBS, sections were counterstained with 300 nmol/l DAPI (Life Technologies) for 15 minutes. Sections were mounted using ProLong Gold Anti-fade mounting medium (Life Technologies).

***Immunohistochemical staining for ILB4, GFAP, VAMP2, and GM2 ganglioside.*** Sections were blocked in 3% $H_2O_2$ in TBS, followed by blocking in 10% normal serum in 0.1% Triton X-100 in TBS for 30 minutes, then incubated overnight at 4 °C with rabbit anti-GFAP (1:500; DakoCytomation, Ely, UK) or chicken anti-VAMP2 (1:500; Millipore) or anti-GM2 antibody (1:40; a gift from Dr Konstantin Dobrenis and Prof Steven Walkey), or peroxidase-conjugated ILB4 from *Bandeiraea simplicifolia* (1:100; Sigma-Aldrich) in blocking solution, washed 4× in TBS, and, with exception for ILB4, stained with the appropriate biotinylated secondary antibody (Vector Laboratories, Burlingame, CA) for 2 hours. After washing with TBS, sections were incubated with avidin-biotin complex (1:200; Vector Laboratories) for 1.5 hours and developed using DAB substrate (Vector Laboratories). To obtain black staining, nickel was added to the DAB substrate buffer. For ILB4 staining, 1 mmol/l $MgCl_2$ and $CaCl_2$ were added to the buffers. Sections were mounted onto positively charged slides (Fisher Scientific) and cover-slipped in DPX medium (Fisher Scientific).

***Statistical analysis.*** JMP software (SAS Institute, Cary, NC) was used with one way analysis of variance and Tukey *post hoc* test for analysis. Where standard deviations were unequal, data were log transformed to achieve normal distributions. Significance was assumed at $P < 0.05$.

## SUPPLEMENTARY MATERIAL

**Figure S1.** LV-eGFP transduction does not affect colony-forming units, lineage distribution, or brain engraftment.

**Figure S2.** Additional tests on LV-PGK-SGSH and LV-CD11b-SGSH.

**Figure S3.** Low power images of isolectin B4 (microglia) staining in WT, MPSIIIA, LV-CD11b– and LV-PGK–treated MPSIIIA mouse brain.

**Figure S4.** Low power images of secondary storage of GM2 ganglioside in WT, MPSIIIA, LV-CD11b– and LV-PGK–treated MPSIIIA mouse brain.

**Video S1.** LV-CD11b but not LV-PGK–modified autologous HSCs correct MPSIIIA mouse behavior.

## ACKNOWLEDGMENTS

This work was funded by the Sanfilippo Children's Research Foundation, The United Kingdom Society for Mucopolysaccharide Diseases, The Irish Society for Mucopolysaccharide Diseases, the BBSRC, CMFT, and the Manchester Biomedical Research Centre. A.S. was a Manchester BRC fellow. The sponsors did not play a role in study design or execution. The authors thank the staff of the Manchester BSU and Professor Luigi Naldini for the pCCL vector backbone. The authors declared no conflict of interest.

## REFERENCES

1. Valstar, MJ, Ruijter, GJ, van Diggelen, OP, Poorthuis, BJ and Wijburg, FA (2008). Sanfilippo syndrome: a mini-review. *J Inherit Metab Dis* **31**: 240–252.
2. Holley, RJ, Deligny, A, Wei, W, Watson, HA, Niñonuevo, MR, Dagälv, A *et al.* (2011). Mucopolysaccharidosis type I, unique structure of accumulated heparan sulfate and increased N-sulfotransferase activity in mice lacking α-L-iduronidase. *J Biol Chem* **286**: 37515–37524.
3. Langford-Smith, A, Wilkinson, FL, Langford-Smith, KJ, Holley, RJ, Sergijenko, A, Howe, SJ *et al.* (2012). Hematopoietic stem cell and gene therapy corrects primary neuropathology and behavior in mucopolysaccharidosis IIIA mice. *Mol Ther* **20**: 1610–1621.
4. Wilkinson, FL, Holley, RJ, Langford-Smith, KJ, Badrinath, S, Liao, A, Langford-Smith, A *et al.* (2012). Neuropathology in mouse models of mucopolysaccharidosis type I, IIIA and IIIB. *PLoS ONE* **7**: e35787.
5. Héron, B, Mikaeloff, Y, Froissart, R, Caridade, G, Maire, I, Caillaud, C *et al.* (2011). Incidence and natural history of mucopolysaccharidosis type III in France and comparison with United Kingdom and Greece. *Am J Med Genet A* **155A**: 58–68.
6. Meyer, A, Kossow, K, Gal, A, Mühlhausen, C, Ullrich, K, Braulke, T *et al.* (2007). Scoring evaluation of the natural course of mucopolysaccharidosis type IIIA (Sanfilippo syndrome type A). *Pediatrics* **120**: e1255–e1261.
7. Bhaumik, M, Muller, VJ, Rozaklis, T, Johnson, L, Dobrenis, K, Bhattacharyya, R *et al.* (1999). A mouse model for mucopolysaccharidosis type III A (Sanfilippo syndrome). *Glycobiology* **9**: 1389–1396.
8. McGlynn, R, Dobrenis, K and Walkley, SU (2004). Differential subcellular localization of cholesterol, gangliosides, and glycosaminoglycans in murine models of mucopolysaccharide storage disorders. *J Comp Neurol* **480**: 415–426.
9. Arfi, A, Richard, M, Gandolphe, C, Bonnefont-Rousselot, D, Thérond, P and Scherman, D (2011). Neuroinflammatory and oxidative stress phenomena in MPS IIIA mouse model: the positive effect of long-term aspirin treatment. *Mol Genet Metab* **103**: 18–25.
10. Fraldi, A, Hemsley, K, Crawley, A, Lombardi, A, Lau, A, Sutherland, L *et al.* (2007). Functional correction of CNS lesions in an MPS-IIIA mouse model by intracerebral AAV-mediated delivery of sulfamidase and SUMF1 genes. *Hum Mol Genet* **16**: 2693–2702.
11. Ruzo, A, Marcó, S, García, M, Villacampa, P, Ribera, A, Ayuso, E *et al.* (2012). Correction of pathological accumulation of glycosaminoglycans in central nervous system and peripheral tissues of MPSIIIA mice through systemic AAV9 gene transfer. *Hum Gene Ther* **23**: 1237–1246.
12. Savas, PS, Hemsley, KM and Hopwood, JJ (2004). Intracerebral injection of sulfamidase delays neuropathology in murine MPS-IIIA. *Mol Genet Metab* **82**: 273–285.
13. Boelens, JJ, Rocha, V, Aldenhoven, M, Wynn, R, O'Meara, A, Michel, G *et al.*; EUROCORD, Inborn error Working Party of EBMT and Duke University. (2009). Risk factor analysis of outcomes after unrelated cord blood transplantation in patients with Hurler syndrome. *Biol Blood Marrow Transplant* **15**: 618–625.
14. Boelens, JJ, Wynn, RF, O'Meara, A, Veys, P, Bertrand, Y, Souillet, G *et al.* (2007). Outcomes of hematopoietic stem cell transplantation for Hurler's syndrome in Europe: a risk factor analysis for graft failure. *Bone Marrow Transplant* **40**: 225–233.
15. Saif, MA, Bigger, BW, Brookes, KE, Mercer, J, Tylee, KL, Church, HJ *et al.* (2012). Hematopoietic stem cell transplantation improves the high incidence of neutralizing allo-antibodies observed in Hurler's syndrome after pharmacological enzyme replacement therapy. *Haematologica* **97**: 1320–1328.
16. Wynn, RF, Wraith, JE, Mercer, J, O'Meara, A, Tylee, K, Thornley, M *et al.* (2009). Improved metabolic correction in patients with lysosomal storage disease treated with hematopoietic stem cell transplant compared with enzyme replacement therapy. *J Pediatr* **154**: 609–611.
17. Krivit, W, Sung, JH, Shapiro, EG and Lockman, LA (1995). Microglia: the effector cell for reconstitution of the central nervous system following bone marrow transplantation for lysosomal and peroxisomal storage diseases. *Cell Transplant* **4**: 385–392.
18. Prasad, VK, Mendizabal, A, Parikh, SH, Szabolcs, P, Driscoll, TA, Page, K *et al.* (2008). Unrelated donor umbilical cord blood transplantation for inherited metabolic disorders in 159 pediatric patients from a single center: influence of cellular composition of the graft on transplantation outcomes. *Blood* **112**: 2979–2989.
19. Shapiro, EG, Lockman, LA, Balthazor, M and Krivit, W (1995). Neuropsychological outcomes of several storage diseases with and without bone marrow transplantation. *J Inherit Metab Dis* **18**: 413–429.
20. Sivakumur, P and Wraith, JE (1999). Bone marrow transplantation in mucopolysaccharidosis type IIIA: a comparison of an early treated patient with his untreated sibling. *J Inherit Metab Dis* **22**: 849–850.
21. Visigalli, I, Delai, S, Politi, LS, Di Domenico, C, Cerri, F, Mrak, E *et al.* (2010). Gene therapy augments the efficacy of hematopoietic cell transplantation and fully corrects mucopolysaccharidosis type I phenotype in the mouse model. *Blood* **116**: 5130–5139.

22. Biffi, A, Capotondo, A, Fasano, S, del Carro, U, Marchesini, S, Azuma, H *et al.* (2006). Gene therapy of metachromatic leukodystrophy reverses neurological damage and deficits in mice. *J Clin Invest* **116**: 3070–3082.
23. Cartier, N, Hacein-Bey-Abina, S, Bartholomae, CC, Veres, G, Schmidt, M, Kutschera, I *et al.* (2009). Hematopoietic stem cell gene therapy with a lentiviral vector in X-linked adrenoleukodystrophy. *Science* **326**: 818–823.
24. Dull, T, Zufferey, R, Kelly, M, Mandel, RJ, Nguyen, M, Trono, D *et al.* (1998). A third-generation lentivirus vector with a conditional packaging system. *J Virol* **72**: 8463–8471.
25. Agura, ED, Howard, M and Collins, SJ (1992). Identification and sequence analysis of the promoter for the leukocyte integrin β-subunit (CD18): a retinoic acid-inducible gene. *Blood* **79**: 602–609.
26. Hickstein, DD, Baker, DM, Gollahon, KA and Back, AL (1992). Identification of the promoter of the myelomonocytic leukocyte integrin CD11b. *Proc Natl Acad Sci USA* **89**: 2105–2109.
27. Langford-Smith, A, Langford-Smith, KJ, Jones, SA, Wynn, RF, Wraith, JE, Wilkinson, FL *et al.* (2011). Female mucopolysaccharidosis IIIA mice exhibit hyperactivity and a reduced sense of danger in the open field test. *PLoS ONE* **6**: e25717.
28. Sardiello, M, Palmieri, M, di Ronza, A, Medina, DL, Valenza, M, Gennarino, VA *et al.* (2009). A gene network regulating lysosomal biogenesis and function. *Science* **325**: 473–477.
29. Cohen, MJ, Park, YD, Kim, H and Pillai, JJ (2010). Long-term neuropsychological follow-up of a child with Klüver-Bucy syndrome. *Epilepsy Behav* **19**: 643–646.
30. Malik, P, Krall, WJ, Yu, XJ, Zhou, C and Kohn, DB (1995). Retroviral-mediated gene expression in human myelomonocytic cells: a comparison of hematopoietic cell promoters to viral promoters. *Blood* **86**: 2993–3005.
31. Rozaklis, T, Beard, H, Hassiotis, S, Garcia, AR, Tonini, M, Luck, A *et al.* (2011). Impact of high-dose, chemically modified sulfamidase on pathology in a murine model of MPS IIIA. *Exp Neurol* **230**: 123–130.
32. Gaspar, HB, Cooray, S, Gilmour, KC, Parsley, KL, Zhang, F, Adams, S *et al.* (2011). Hematopoietic stem cell gene therapy for adenosine deaminase-deficient severe combined immunodeficiency leads to long-term immunological recovery and metabolic correction. *Sci Transl Med* **3**: 97–80.
33. Ausseil, J, Desmaris, N, Bigou, S, Attali, R, Corbineau, S, Vitry, S *et al.* (2008). Early neurodegeneration progresses independently of microglial activation by heparan sulfate in the brain of mucopolysaccharidosis IIIB mice. *PLoS ONE* **3**: e2296.
34. Piccinini, AM and Midwood, KS (2010). DAMPening inflammation by modulating TLR signalling. *Mediators Inflamm* (epub ahead of print).
35. Archer, LD, Langford-Smith, KJ, Bigger, BW, and Fildes, JE (2013). Mucopolysaccharide diseases: a complex interplay between neuroinflammation, microglial activation and adaptive immunity. *J Inherit Metab Dis* (epub ahead of print).
36. Langford-Smith, KJ, Mercer, J, Petty, J, Tylee, K, Church, H, Roberts, J *et al.* (2011). Heparin cofactor II-thrombin complex and dermatan sulphate:chondroitin sulphate ratio are biomarkers of short- and long-term treatment effects in mucopolysaccharide diseases. *J Inherit Metab Dis* **34**: 499–508.
37. Langford-Smith, K, Arasaradnam, M, Wraith, JE, Wynn, R and Bigger, BW (2010). Evaluation of heparin cofactor II-thrombin complex as a biomarker on blood spots from mucopolysaccharidosis I, IIIA and IIIB mice. *Mol Genet Metab* **99**: 269–274.
38. de Ruijter, J, de Ru, MH, Wagemans, T, Ijlst, L, Lund, AM, Orchard, PJ *et al.* (2012). Heparan sulfate and dermatan sulfate derived disaccharides are sensitive markers for newborn screening for mucopolysaccharidoses types I, II and III. *Mol Genet Metab* **107**: 705–710.
39. de Ru, MH, van der Tol, L, van Vlies, N, Bigger, BW, Hollak, CE, Ijlst, L *et al.* (2013). Plasma and urinary levels of dermatan sulfate and heparan sulfate derived disaccharides after long-term enzyme replacement therapy (ERT) in MPS I: correlation with the timing of ERT and with total urinary excretion of glycosaminoglycans. *J Inherit Metab Dis* **36**: 247–255.
40. Wilkinson, FL, Sergijenko, A, Langford-Smith, KJ, Malinowska, M, Wynn, RF and Bigger, BW (2013). Busulfan conditioning enhances engraftment of hematopoietic donor-derived cells in the brain compared with irradiation. *Mol Ther* **21**: 868–876.
41. Capotondo, A, Milazzo, R, Politi, LS, Quattrini, A, Palini, A, Plati, T *et al.* (2012). Brain conditioning is instrumental for successful microglia reconstitution following hematopoietic stem cell transplantation. *Proc Natl Acad Sci USA* **109**: 15018–15023.
42. Gentner, B, Visigalli, I, Hiramatsu, H, Lechman, E, Ungari, S, Giustacchini, A *et al.* (2010). Identification of hematopoietic stem cell-specific miRNAs enables gene therapy of globoid cell leukodystrophy. *Sci Transl Med* **2**: 58–84.
43. Zanta-Boussif, MA, Charrier, S, Brice-Ouzet, A, Martin, S, Opolon, P, Thrasher, AJ *et al.* (2009). Validation of a mutated PRE sequence allowing high and sustained transgene expression while abrogating WHV-X protein synthesis: application to the gene therapy of WAS. *Gene Ther* **16**(*5*): 605–619.
44. Bigger, BW, Siapati, EK, Mistry, A, Waddington, SN, Nivsarkar, MS, Jacobs, L *et al.* (2006). Permanent partial phenotypic correction and tolerance in a mouse model of hemophilia B by stem cell gene delivery of human factor IX. *Gene Ther* **13**: 117–126.
45. Siapati, EK, Bigger, BW, Miskin, J, Chipchase, D, Parsley, KL, Mitrophanous, K *et al.* (2005). Comparison of HIV- and EIAV-based vectors on their efficiency in transducing murine and human hematopoietic repopulating cells. *Mol Ther* **12**: 537
46. Langford-Smith, A, Malinowska, M, Langford-Smith, KJ, Wegrzyn, G, Jones, S, Wynn, R *et al.* (2011). Hyperactive behaviour in the mouse model of mucopolysaccharidosis IIIB in the open field and home cage environments. *Genes Brain Behav* **10**: 673–682.
47. Malinowska, M, Wilkinson, FL, Langford-Smith, KJ, Langford-Smith, A, Brown, JR, Crawford, BE *et al.* (2010). Genistein improves neuropathology and corrects behaviour in a mouse model of neurodegenerative metabolic disease. *PLoS ONE* **5**: e14192.
48. Canal, MM, Wilkinson, FL, Cooper, JD, Wraith, JE, Wynn, R and Bigger, BW (2010). Circadian rhythm and suprachiasmatic nucleus alterations in the mouse model of mucopolysaccharidosis IIIB. *Behav Brain Res* **209**: 212–220.